Supporting Information

Molecular Glue that Spatiotemporally Turns on Protein–Protein Interactions

Rina Mogaki,[†] Kou Okuro,[*,†] Ryosuke Ueki,[†] Shinsuke Sando,[†] and Takuzo Aida[*,†,‡]

[†]*Department of Chemistry and Biotechnology, School of Engineering*

The University of Tokyo,

7-3-1 Hongo, Bunkyo-ku, Tokyo 113-8656, Japan

[‡]*Riken Center for Emergent Matter Science*

2-1 Hirosawa, Wako, Saitama 351-0198, Japan

Table of Contents

1. General

^{1}H and ^{13}C NMR spectra were recorded on a JEOL type JNM-ECA 500II spectrometer, where chemical shifts for ^{1}H NMR spectroscopy were determined with respect to non-deuterated solvent residues; $CHCl_3$ (δ 7.26) and HDO (δ 4.79), and those for ^{13}C NMR spectroscopy were determined with respect to $CDCl_3$ (δ 77.2). Matrix-assisted laser desorption/ionization time-of-flight mass (MALDI-TOF-MS) spectrometry was performed using α-cyano-4-hydroxy cinnamic acid (CCA) or sinapic acid (SA) as a matrix on a Bruker Daltonics Autoflex™ Speed MALDI-TOF/TOF spectrometer. Recycling preparative gel permeation chromatography (GPC) was performed on a Japan Analytical Industry model LC-918 high performance liquid chromatography using a column set consisting of JAIGEL 1H, 2H, and 2.5H. Normal-phase column chromatography was performed using Merck alumina 90 standardized. Photoirradiation was performed on an Optocode model LED-EXHD light-emitting diode (LED) light source equipped with a 365-nm LED lamp (EX-365). Phase-contrast and confocal laser scanning microscopies were performed on a Leica model TCS SP8 confocal laser-scanning microscope. Image analysis of immunoblotting membranes was performed on an ATTO model AE-9300H luminescent image analyzer. Image analysis of thin layer chromatography (TLC) plates was performed on a FUJIFILM model LAS-3000 luminescent image analyzer. Electronic absorption spectra were recorded on a JASCO type V-670 spectrophotometer or a Molecular Devices SpectraMax® Paradigm® multi-mode microplate detection platform. Fluorescence spectra were recorded on a JASCO type FP-8500 spectrofluorometer. Zeta potential measurements were performed using a Malvern model Zetasizer Nano ZS particle size analyzer equipped with a 532-nm frequency doubled diode-pumped solid-state (DPSS) laser light source. A Horiba type LAQUAtwin-pH-22B compact pH meter was used for pH measurements.

Unless otherwise noted, reagents and solvents were used as received from commercial sources without further purification. Human prostate carcinoma DU145 cells were obtained from Riken BioResource Research Center under a material transfer agreement. RPMI1640 supplemented with GlutaMAX™ was purchased from Thermo Fisher Scientific. Bovine serum albumin (BSA), Dulbecco's phosphate buffer saline (D-PBS), and ImmunoStar® LD were purchased from FUJIFILM Wako Pure Chemical Corporation. Fetal bovine serum (FBS) was purchased from GE Healthcare. Recombinant human hepatocyte growth factor (HGF) was purchased from PeproTech. Rabbit monoclonal antibodies (mAb) for phospho-Met (Tyr1234/1235; #3077), Met (#8198), and beta-actin (#4967) were purchased from Cell Signaling

Technology. Polyclonal goat anti-rabbit immunoglobulins/HRP (#P0488) was purchased from Agilent. HEPES (1.0 M) buffer solution (pH 7.3) and Cell Counting Kit-8 were purchased from Dojindo. Triton™ X-100 was purchased from Sigma-Aldrich. Protease Inhibitor Cocktail and Phosphatase Inhibitor Cocktail were purchased from Nacalai Tesque. A CellBrite Orange cytoplasmic membrane-labeling kit was purchased from Biotium, Inc.

2. Synthesis

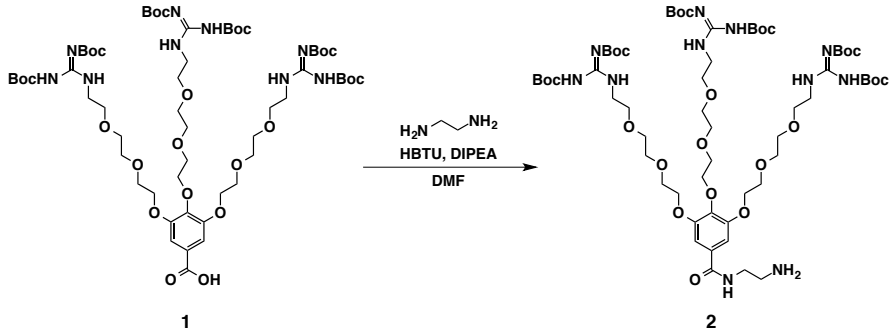

Compound 2. To a DMF (0.50 mL) solution of ethylenediamine (100 mg, 1.66 mmol) was dropwisely added a DMF (0.90 mL) solution of a mixture of **1**[S1] (200 mg, 0.155 mmol), *o*-(benzotriazol-1-yl)-*N*,*N*,*N*',*N*'-tetramethyluronium hexafluorophosphate (HBTU, 62 mg, 0.164 mmol), and diisopropylethylamine (DIPEA, 40 μL, 0.232 mmol), and the mixture was stirred for 17 h at room temperature. The reaction mixture was diluted with AcOEt (10 mL) and washed with water (10 mL × 2) followed by brine (10 mL). An organic extract separated was dried over Na_2SO_4 and filtered off from an insoluble fraction. The filtrate was evaporated to dryness under reduced pressure, and the residue was chromatographed on alumina with AcOEt/MeOH (9/1 to 0/1) as an eluent to allow isolation of **2** as pale yellow oil (67 mg, 32%). ^{1}H NMR (500 MHz; $CDCl_3$; ppm): δ 1.45–1.50 (m, 54H; $C(CH_3)_3$), 2.92 (t, J = 5.8 Hz, 2H; CH_2NH_2), 3.45–3.48 (m, 2H; ArCONHCH_2), 3.55–3.89 (m, 30H; OCH_2, CH_2NHCN), 4.20–4.22 (m, 6H; $ArOCH_2$), 7.10 (s, 2H; ArH), 8.60 (br, 3H; CH_2N*H*CN), 11.46 (br, 3H; $NHCO_2$). ^{13}C NMR (126 MHz; $CDCl_3$; ppm): δ 28.2, 28.4, 40.7, 41.6, 42.9, 69.0, 69.5, 69.9, 70.5, 70.8, 72.4, 79.4, 83.2, 107.2, 129.0, 131.1, 152.5, 153.1, 156.4. MALDI-TOF-MS (CCA): m/z found: 732.97 ([M – 6Boc + H^+] calcd: 732.44).

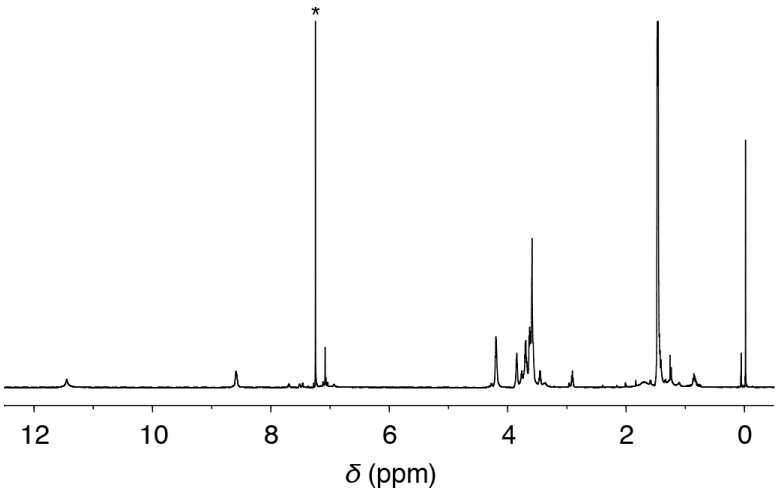

Figure S1. ^{1}H NMR spectrum of **2** in $CDCl_3$ at 21 °C. The signal marked with an asterisk at δ 7.26 ppm is due to $CHCl_3$.

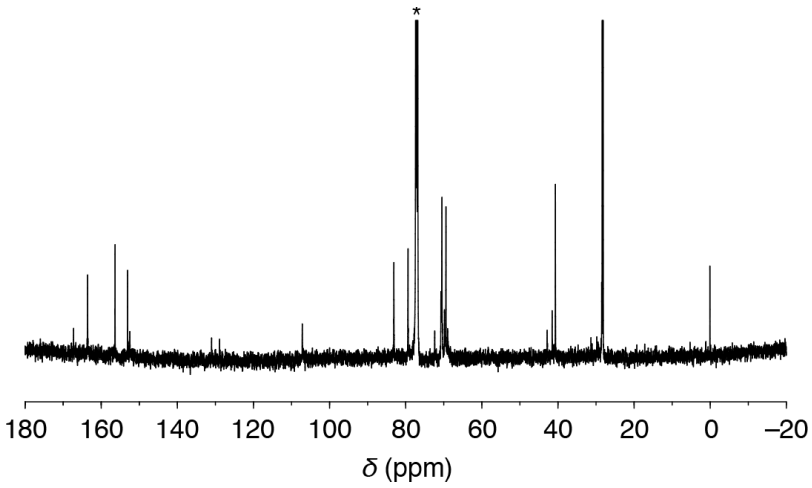

Figure S2. ^{13}C NMR spectrum of **2** in $CDCl_3$ at 21 °C. The signal marked with an asterisk at δ 77.2 ppm is due to $CDCl_3$.

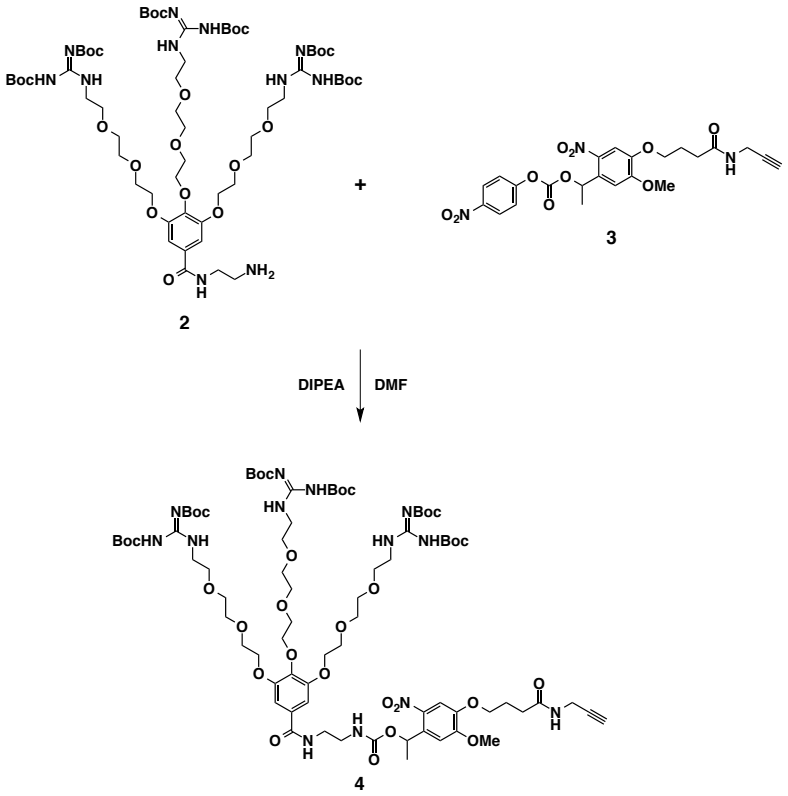

Compound 4. To a DMF (0.80 mL) solution of a mixture of **2** (67 mg, 50 μmol) and **3**[S2] (38 mg, 76 μmol) was added diisopropylethylamine (DIPEA, 11 μL, 60 μmol), and the mixture was stirred for 3 h at room temperature. The reaction mixture was diluted with CH_2Cl_2 (5 mL) and washed with water (5 mL × 2) followed by brine (5 mL). An organic extract separated was dried over Na_2SO_4 and filtered off from an insoluble fraction. The filtrate was evaporated to dryness under reduced pressure, and the residue was subjected to recycling preparative GPC with $CHCl_3$ as an eluent to allow isolation of **4** as pale yellow oil (37 mg, 43%). ^{1}H NMR (500 MHz; $CDCl_3$; ppm): δ 1.45–1.51 (m, 54H; $C(CH_3)_3$), 1.86 (br, 3H; $CHCH_3$), 2.14–2.22 (m, 2H; $CH_2CH_2CH_2$), 2.23 (t, J = 2.3 Hz, 1H; CH_2CCH), 2.42–2.45 (m, 2H; $COCH_2$), 3.53–4.24 (m, 47H; OCH_2, $ArOCH_2$, $ArOCH_3$, CH_2NHCN, CH_2NHCO_2, $ArCONHCH_2$, CH_2CCH), 5.61 (t, J = 5.8 Hz, 1H; CH_2CONH), 6.33–6.36 (m, 1H; $ArCH(CH_3)$), 6.48 (br, 1H; ArCONH), 6.86 (s, 1H; ArH), 6.93 (s, 2H; ArH), 7.48 (s, 1H; ArH), 8.61 (br, 3H; CH_2NHCN), 11.47 (s, 3H; $NHCO_2$). ^{13}C NMR (126 MHz; $CDCl_3$; ppm): δ 22.4, 24.9, 28.2, 28.4, 29.2, 32.7, 36.6, 40.7, 41.2, 56.3, 68.5, 68.8, 69.2, 69.4, 69.9, 70.5, 70.8, 71.5, 72.4, 79.4, 80.1, 83.2, 106.5, 107.5, 109.0, 129.0, 134.2, 139.3, 141.1, 147.1, 152.5, 153.1, 154.1, 156.4, 162.7, 163.6, 167.7, 172.2. MALDI-TOF-MS (CCA): m/z found: 1094.94 ([M – 6Boc + H^+] calcd: 1094.55).

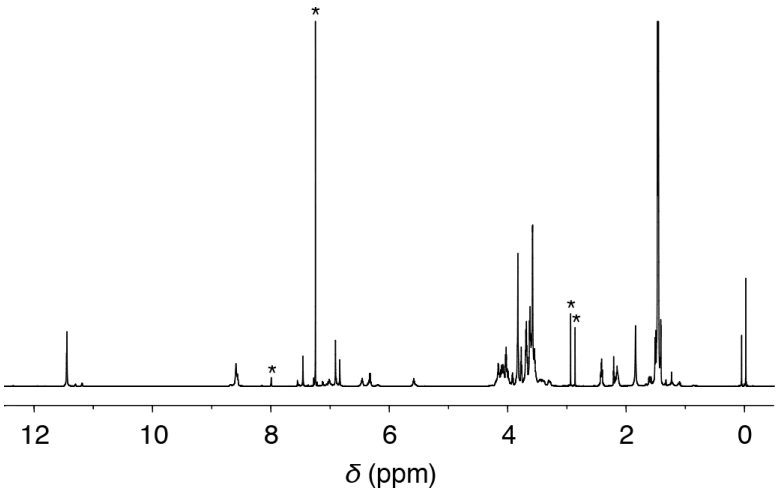

Figure S3. ^{1}H NMR spectrum of **4** in $CDCl_3$ at 21 °C. The signals marked with asterisks at δ 7.26 ppm and δ 2.88, 2.96, and 8.01 ppm are due to $CHCl_3$ and DMF, respectively.

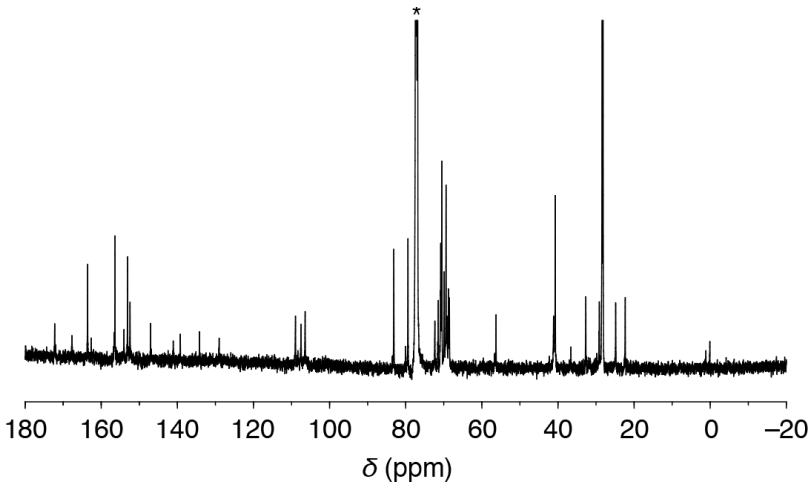

Figure S4. ^{13}C NMR spectrum of **4** in $CDCl_3$ at 21 °C. The signal marked with an asterisk at δ 77.2 ppm is due to $CDCl_3$.

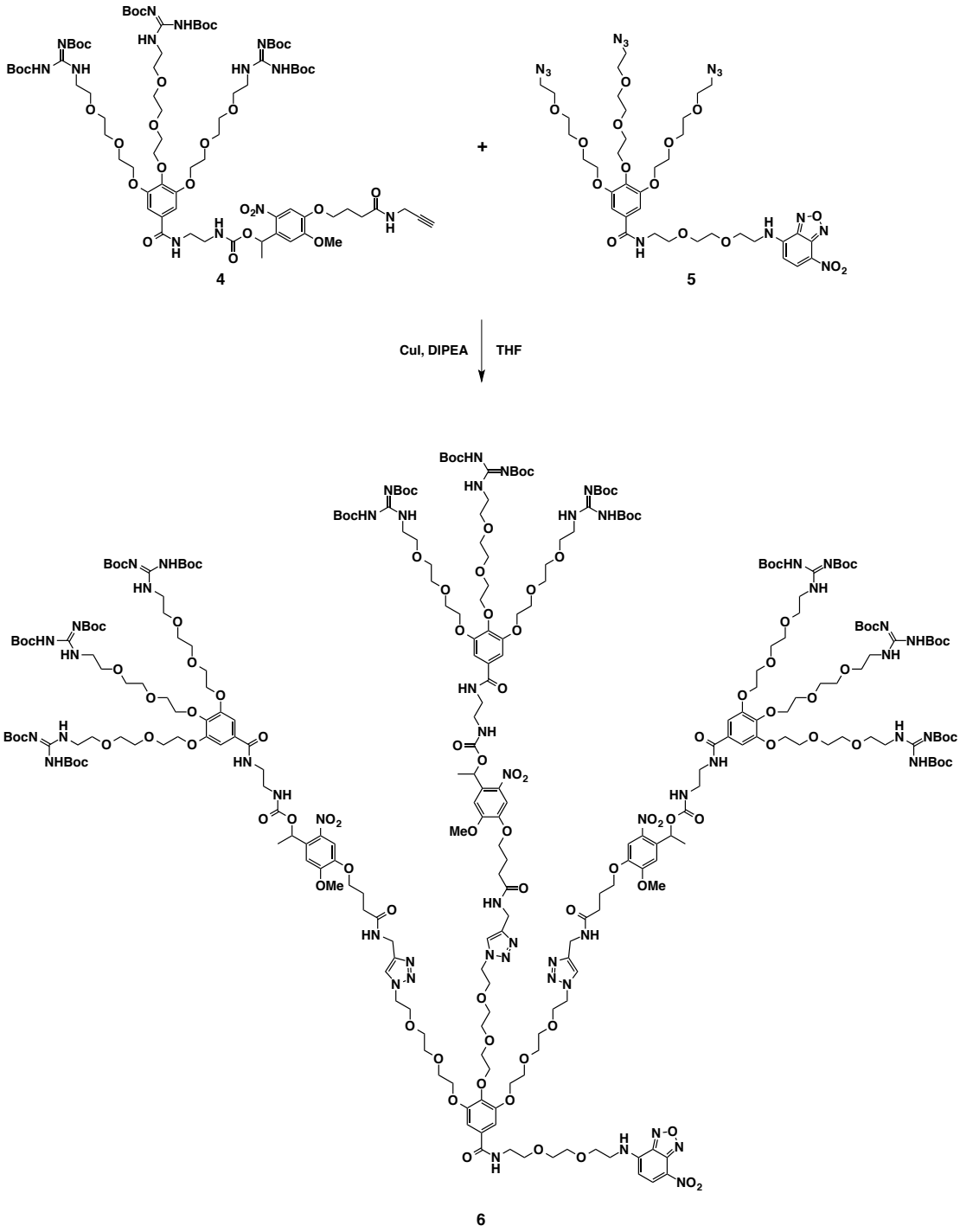

Compound 6. To a THF (0.70 mL) solution of a mixture of **4** (37 mg, 22 μmol), **5**[S3] (6.1 mg, 6.5 μmol), and diisopropylethylamine (DIPEA, 5.0 μL, 29 μmol) was added copper(I) iodide (CuI,

7.8 mg, 41 μmol), and the mixture was stirred for 22 h at room temperature. Then, THF (0.30 mL), CuI (2.1 mg, 11 μmol), and DIPEA (2.0 μL, 12 μmol) were successively added to the reaction mixture, and the resultant suspension was stirred for 20 h at room temperature. Then, $CHCl_3$ (1 mL) was added to the resultant mixture and filtered off with celite from an insoluble fraction. The filtrate was evaporated to dryness under reduced pressure, and the residue was dissolved in $CHCl_3$ (2 mL) and washed with saturated aqueous NH_4Cl (2 mL × 2) followed by brine (2 mL). An organic extract separated was dried over Na_2SO_4 and filtered off from an insoluble fraction. The filtrate was evaporated to dryness under reduced pressure, and the residue was subjected to recycling preparative GPC with $CHCl_3$ as an eluent to allow isolation of **6** as pale orange oil (9.1 mg, 23%). ^{1}H NMR (500 MHz; $CDCl_3$; ppm): δ 1.45–1.50 (m, 162H; $C(CH_3)_3$), 1.80 (br, 9H; $CHCH_3$), 2.10–2.16 (m, 6H; $CH_2CH_2CH_2$), 2.39 (t, J = 6.8 Hz, 6H; $COCH_2$), 3.32–4.24 (m, 183H; OCH_2, $ArOCH_2$, $ArOCH_3$, CH_2NH), 4.41–4.47 (m, 12H; triazole-CH_2NH, OCH_2CH_2-triazole), 5.88 (br, 2H; $ArCONHCH_2CH_2O$, CH_2NH-NBD), 6.10 (br, 1H; NBD), 6.30–6.34 (m, 3H; $ArCH(CH_3)$), 6.92 (s, 3H; ArH), 7.07 (s, 8H; ArH), 7.47 (s, 3H; ArH), 7.70 (s, 3H; triazole-H), 8.38 (d, J = 4.3 Hz, 1H; NBD), 8.56–8.65 (m, 9H; CH_2NHCN), 11.46 (s, 9H; $NHCO_2$). ^{13}C NMR (126 MHz; $CDCl_3$; ppm): δ 22.4, 24.9, 28.2, 28.4, 32.6, 35.1, 40.7, 41.0, 41.5, 50.3, 56.4, 69.0, 69.4, 70.0, 70.5, 70.6, 70.9, 72.5, 79.4, 83.1, 83.2, 106.9, 108.1, 108.9, 123.5, 129.1, 134.1, 139.5, 141.5, 144.7, 147.1, 152.6, 153.1, 154.1, 156.4, 163.6, 167.8, 172.5.

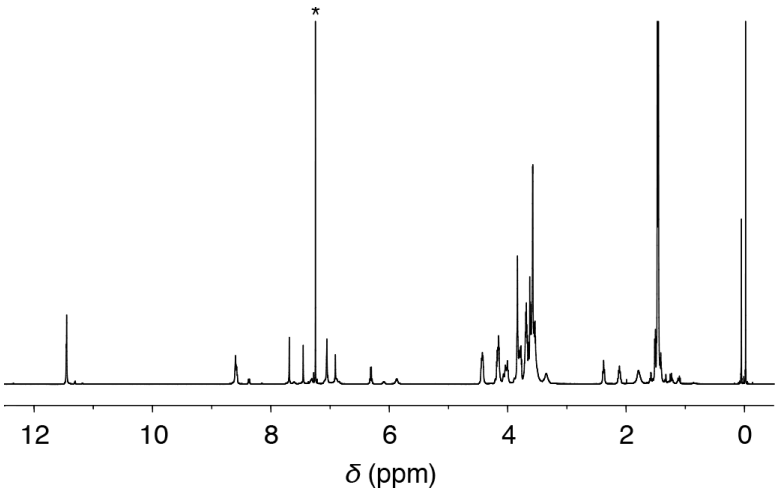

Figure S5. ^{1}H NMR spectrum of **6** in $CDCl_3$ at 21 °C. The signal marked with an asterisk at δ 7.26 ppm is due to $CHCl_3$.

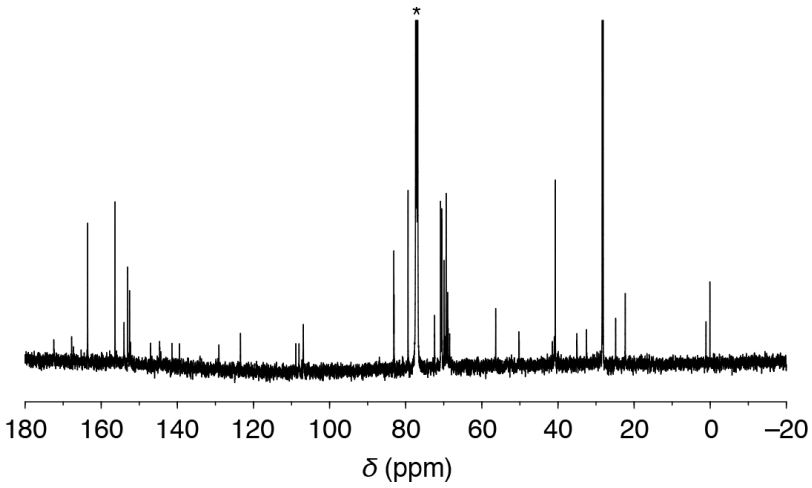

Figure S6. ^{13}C NMR spectrum of **6** in $CDCl_3$ at 21 °C. The signal marked with an asterisk at δ 77.2 ppm is due to $CDCl_3$.

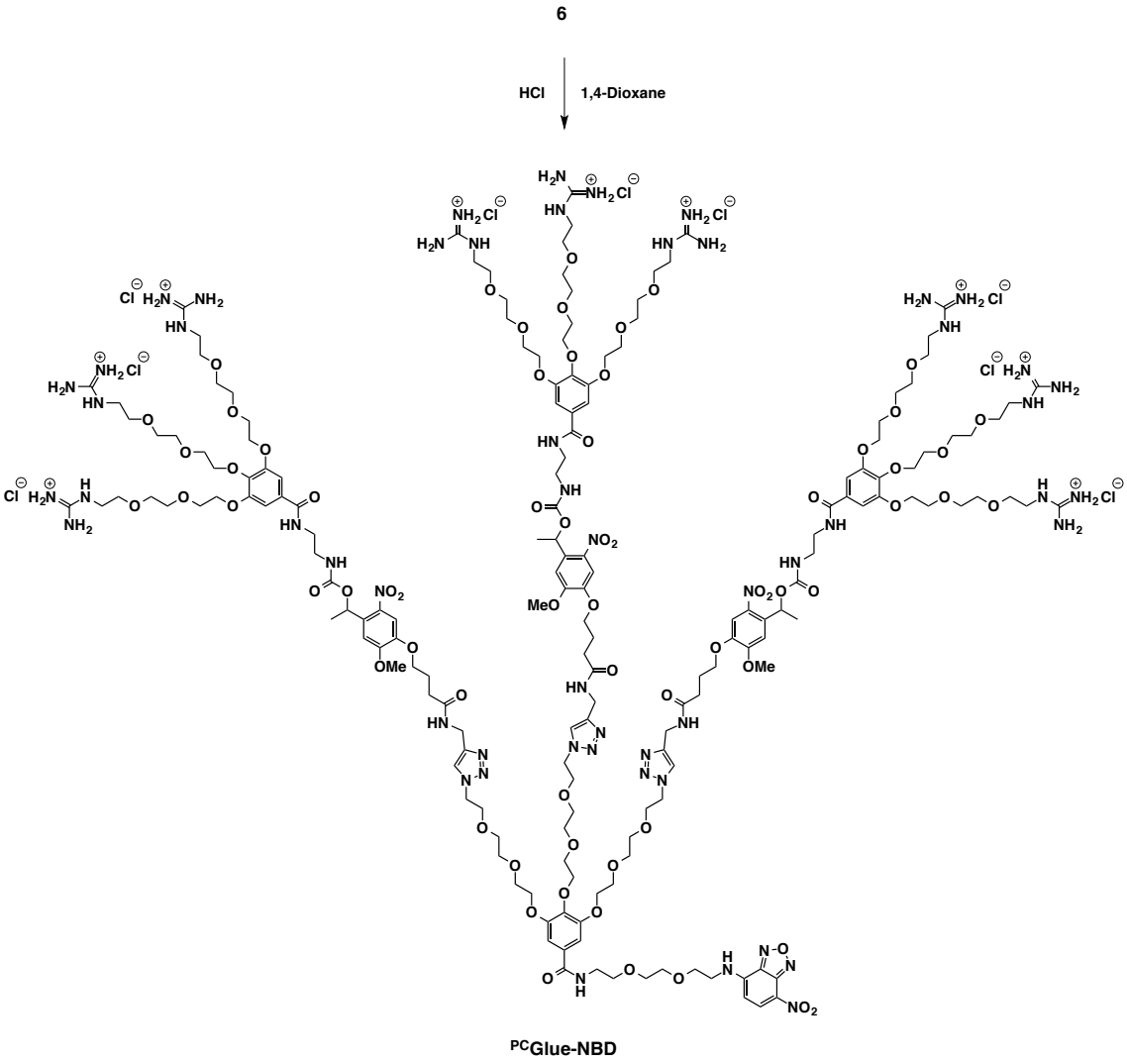

^{PC}Glue-NBD. A 1,4-dioxane (4 mL) solution of HCl (4 M) was added to **6** (9.1 mg, 1.5 μmol), and the mixture was stirred overnight at room temperature. Then, the resultant mixture was reprecipitated with hexane to allow isolation of **^{PC}Glue-NBD** as orange oil (7.8 mg, quant.). ^{1}H NMR (500 MHz; D_2O; ppm): δ 1.32 (br, 9H; CHC*H*$_3$), 1.95 (br, 6H; $CH_2CH_2CH_2$), 2.32 (br, 6H; $COCH_2$), 3.14–4.53 (m, 189H; OCH_2, $ArOCH_2$, $ArOCH_3$, C*H*$_2$NH, triazole-C*H*$_2$NH, OCH_2CH_2-triazole), 6.04 (br, 4H; ArC*H*(CH_3), NBD), 6.68–7.19 (m, 14H; ArH), 7.86 (br, 3H; triazole-H), 7.98 (br, 1H; NBD). ^{13}C NMR (126 MHz; D_2O; ppm): δ 21.8, 25.2, 32.6, 34.5, 41.9, 43.8, 60.9, 63.1, 66.6, 67.2, 67.8, 68.7, 69.5, 70.4, 72.2, 106.0, 124.7, 139.5, 145.1, 152.3, 157.8. MALDI-TOF-MS (SA): *m*/*z* found: 4214.02 ([M – 9HCl + H$^+$] calcd: 4216.02).

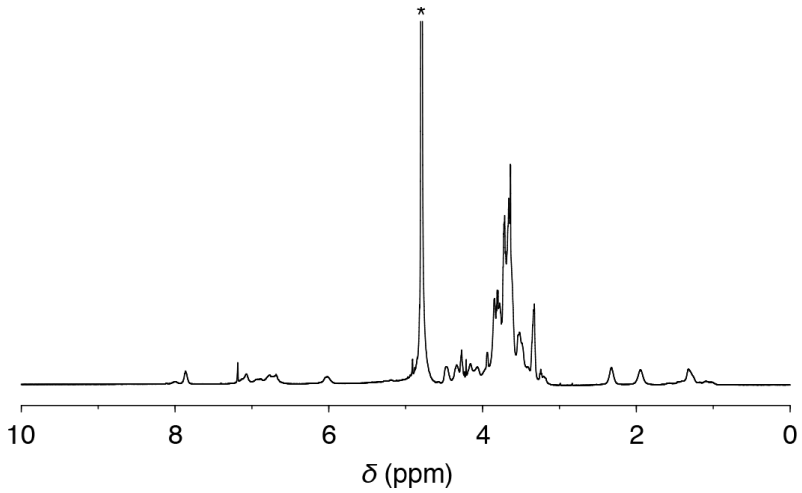

Figure S7. ^{1}H NMR spectrum of ^{PC}Glue-NBD in D_2O at 21 °C. The signal marked with an asterisk at δ 4.79 ppm is due to water.

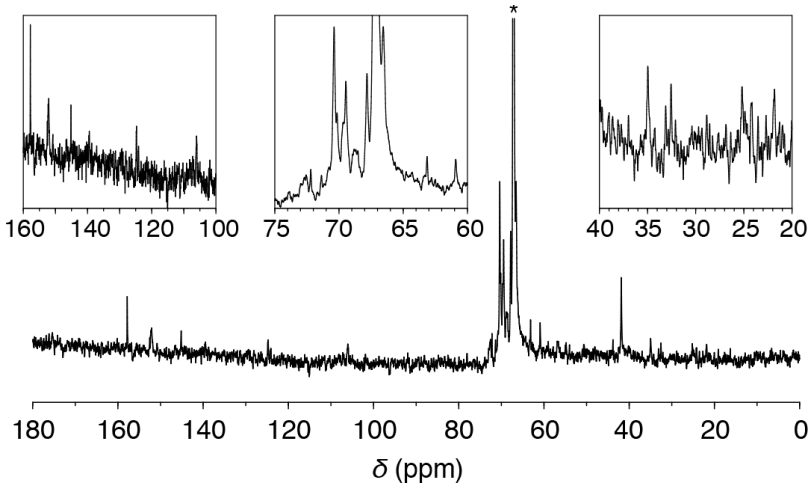

Figure S8. ^{13}C NMR spectrum of ^{PC}Glue-NBD in D_2O at 21 °C. The signal marked with an asterisk at δ 67.2 ppm is due to 1,4-dioxane as an internal standard. The insets show magnified spectra at δ 20–40 ppm, δ 60–75 ppm, and δ 100–160 ppm, respectively.

3. Electronic Absorption Spectroscopy

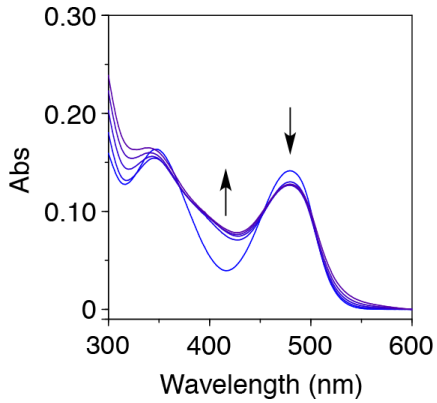

Figure S9. Absorption spectral changes of ^{PC}Glue-NBD (10 μM) at 37 °C in HEPES buffer (50 mM, pH 7.2) upon photoirradiation at 365 nm (0–2 min, 1.1 mW/mm^2).

4. Thin Layer Chromatography (TLC) Analysis

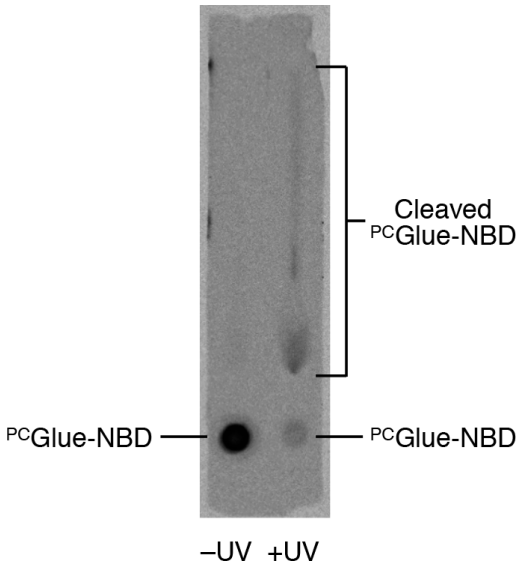

Figure S10. TLC profiles (eluent: CH_2Cl_2/MeOH = 7/3; λ_{ex} = 470 nm) of ^{PC}Glue-NBD (10 μM) before and after exposure to UV light at 365 nm (1.1 mW/mm^2) for 2 min in water. ^{PC}Glue-NBD was photocleaved in 82% conversion, as estimated by image analysis of the TLC plate.

5. Fluorescence Spectral Titration

The association constant (K_{assoc}) was determined based on the Hill equation, by plotting the fractions of bound ^{PC}Glue-NBD against the concentrations of bovine serum albumin (BSA). The fractions of bound ^{PC}Glue-NBD (θ) were calculated from $(I - I_0)/(I_{sat} - I_0)$, where I_0, I, and I_{sat} represent the fluorescence intensities at 540 nm before titration, observed with BSA, and at the saturation point, respectively. The data were then fit to the Hill equation: $\theta = [BSA]^n/((K_d)^n + [BSA]^n)$, where [BSA] is the concentration of BSA, K_d (= $1/K_{assoc}$) is the dissociation constant, and n is the Hill coefficient.[S4,S5] The estimated K_{assoc} and n were 6.3×10^5 M^{-1} (EC_{50} = 1.6 μM) and 1.3, respectively.

6. Zeta Potential Measurements

A HEPES buffer (2.5 mM, pH 7.2) solution of a mixture of BSA (20 μM) and ^{PC}Glue-NBD (50 μM) before and after 2 min exposure to UV light (λ = 365 nm) was subjected to zeta potential measurements. Zeta potentials in HEPES buffer (2.5 mM, pH 7.2) of BSA (20 μM) and ^{PC}Glue-NBD (50 μM) were also measured.

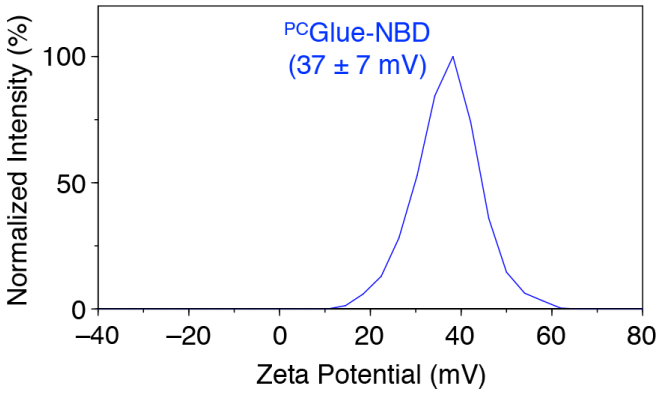

Figure S11. Zeta potential profile at 25 °C of ^{PC}Glue-NBD (50 μM) in HEPES buffer (2.5 mM, pH 7.2).

7. Phase-contrast Microscopy

Human prostate carcinoma DU145 cells (3.4×10^2 cells/well; 8-chambered glass substrate, culture area = 0.8 cm^2) were incubated in RPMI1640 (200 μL) containing 10% fetal bovine serum (FBS) at 37 °C under 5% CO_2 for 4 days. The cell sample was rinsed with Dulbecco's phosphate buffer saline (D-PBS, 200 μL × 2) and supplied with RPMI1640 (0.5% FBS, 200 μL) containing hepatocyte growth factor (HGF, 500 pM) and ^{PC}Glue-NBD (2 μM), which was exposed to UV light (λ = 365 nm, 1.1 mW/mm^2) for 2 min prior to incubation. Then, the cell sample was subjected to phase-contrast microscopy. An analogous cell sample without UV exposure was prepared under conditions otherwise identical to the above procedure. Likewise, reference cell samples in the absence and presence of HGF (500 pM) were prepared under conditions otherwise identical to the above procedures.

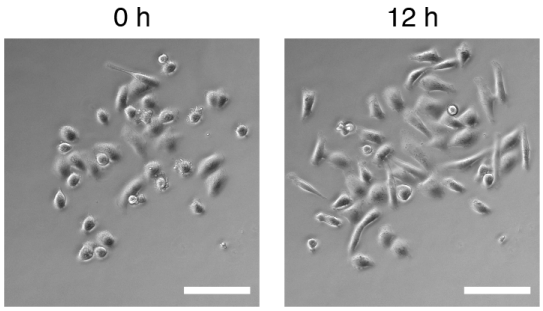

Figure S12. Phase-contrast micrographs of DU145 cells in RPMI1640 (0.5% FBS) at 37 °C. Scale bars = 100 μm.

8. Western Blotting Analysis

8-1. Preparation of Cell Lysates

DU145 cells (1.0×10^5 cells/dish; 40-mm dish, culture area = 12.6 cm^2) were incubated at 37 °C under 5% CO_2 for 24 h in RPMI1640 (10% FBS, 2 mL). The cell sample was rinsed with D-PBS (1 mL), supplied with RPMI1640 (0.5% BSA, 2 mL), and incubated at 37 °C under 5% CO_2 for 24 h. Then, the culture medium was removed, and the cell sample was supplied with RPMI1640 (0.5% BSA, 1 mL) containing HGF (100 pM) and ^{PC}Glue-NBD (5 μM), which was exposed to UV light (λ = 365 nm, 1.1 mW/mm^2) for 2 min prior to incubation. After incubation of the resultant mixture at 37 °C under 5% CO_2 for 15 min, the cell sample was rinsed with D-PBS (700 μL × 2) and supplied with Tris-HCl buffer (20 mM Tris-HCl, 137 mM NaCl, 2 mM EDTA, 1% Triton™ X-100, 10% glycerol, pH 8.0, 150 μL) containing Protease Inhibitor Cocktail and Phosphatase Inhibitor Cocktail. The obtained suspension was collected and incubated on ice for 20 min. Then, the resultant suspension was centrifuged at 10,000 ×g for 20 min at 4 °C. The supernatant was collected as DU145 cell lysates, and the total protein concentration was quantified by bicinchoninic acid (BCA) assay using BSA as a standard.[S6] An analogous cell lysate without UV exposure was prepared under conditions otherwise identical to the above procedure. Likewise, reference cell lysates were prepared using ^{PC}Glue-NBD-free RPMI1640 (0.5% BSA, 1 mL) or ^{PC}Glue-NBD-free RPMI1640 (0.5% BSA, 1 mL) containing HGF (100 pM) under conditions otherwise identical to the above procedures.

8-2. Immunoblotting

DU145 cell lysates (final total protein 2 μg) were subjected to sodium dodecyl sulfate-polyacrylamide gel electrophoresis (SDS-PAGE) and then transferred onto a polyvinylidene fluoride (PVDF) membrane. The membrane was incubated with anti-phospho-Met (Y1234/Y1235) rabbit monoclonal antibody as primary antibody followed by polyclonal goat anti-rabbit immunoglobulins/HRP as secondary antibody according to the previously reported procedure.[S7] Then, the membrane was developed with ImmunoStar® LD according to the procedure provided by the supplier (FUJIFILM Wako Pure Chemical Corporation) and visualized using an ATTO model AE-9300H luminescent image analyzer. Likewise, rabbit monoclonal antibodies for Met and β-actin were used as primary antibodies for detection of total Met (p-Met and c-Met) and β-actin, respectively, under conditions otherwise identical to the above procedure.

9. Confocal Laser Scanning Microscopy

DU145 cells (1.9×10^3 cells/dish; 35-mm glass bottom culture dish, culture area = 5.7 cm^2) were incubated in RPMI1640 (10% FBS, 1 mL) at 37 °C under 5% CO_2 for 4 days. The cell sample was rinsed with D-PBS (1 mL × 2) and incubated for 20 min at 37 °C in RPMI1640 (10% FBS, 1 mL) with 0.5% CellBrite Orange. The cell sample was rinsed with D-PBS (1 mL × 2) and supplied with RPMI1640 (0.5% FBS, 1 mL) containing HGF (500 pM) and ^{PC}Glue-NBD (2 μM). The cell sample was exposed to UV light (λ = 365 nm, 1.1 mW/mm^2) for 2 min through a plastic tape mask (Figure S13) and then subjected to confocal laser scanning microscopy (λ_{ext} = 552 nm). A reference cell sample exposed to UV light (λ = 365 nm, 1.1 mW/mm^2) for 2 min in the absence of HGF was likewise prepared under otherwise identical conditions to the above (Figure S14).

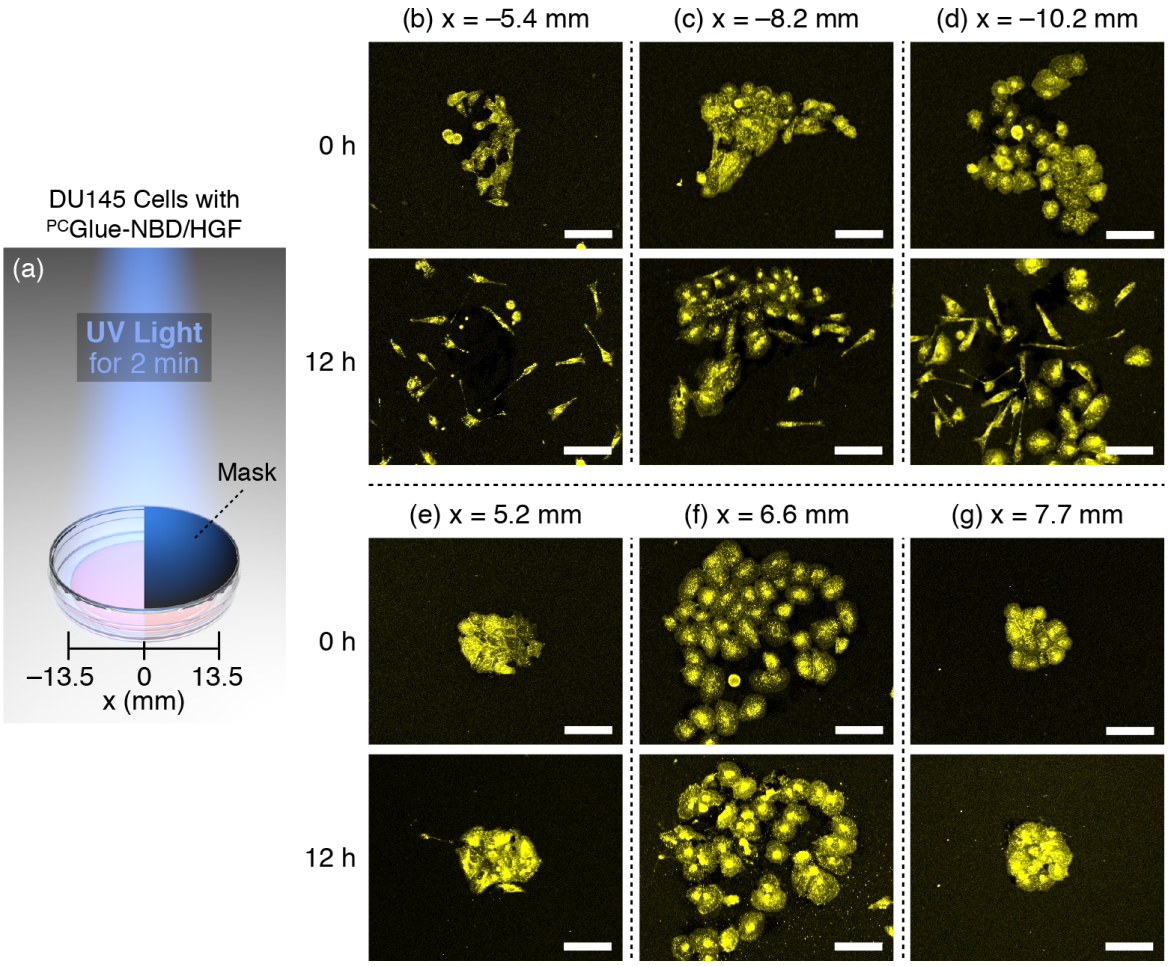

Figure S13. (a) Schematic illustration of the experimental setup for *in situ* turning on the HGF/c-Met interaction using ^{PC}Glue-NBD in the presence of DU145 cells. Left half (x = –13.5–0 mm) and right half (x = 0–13.5 mm) are UV-exposed (365 nm, 2 min, 1.1 mW/mm^2) and non-exposed areas, respectively. (b–g) Confocal laser scanning micrographs (λ_{ex} = 552 nm, λ_{obs} = 560–620 nm) of CellBrite Orange-labeled DU145 cells at 37 °C in RPMI1640 (0.5% FBS) containing ^{PC}Glue-NBD (2 μM) and HGF (500 pM) at (b) x = –5.4, (c) x = –8.2, (d) x = –10.2, (e) x = 5.2, (f) x = 6.6, and (g) x = 7.7 mm. Scale bars = 100 μm.

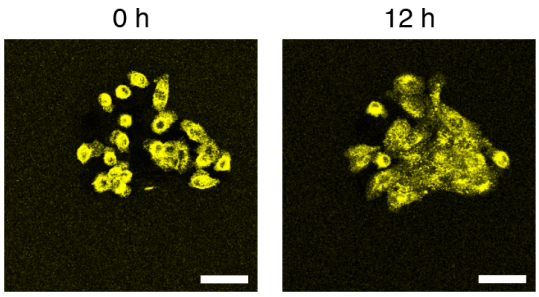

Figure S14. Confocal laser scanning micrographs (λ_{ex} = 552 nm, λ_{obs} = 560–620 nm) of CellBrite Orange-labeled DU145 cells at 37 °C in RPMI1640 (0.5% FBS) after 2 min UV exposure at 365 nm (1.1 mW/mm^2). Scale bars = 100 μm.

10. Cell Viability Assay

DU145 cells (5.0×10^3 cells/well; 96-well culture plate, culture area = 0.33 cm^2/well) were incubated in RPMI1640 (10% FBS, 100 μL) at 37 °C under 5% CO_2 for 24 h. The cell sample was rinsed with D-PBS (100 μL × 2) and supplied with RPMI1640 (0.5% FBS, 100 μL) containing ^{PC}Glue-NBD (0.1–20 μM), which was exposed to UV light (λ = 365 nm, 1.1 mW/mm^2) for 2 min prior to incubation. After incubation at 37 °C under 5% CO_2 for 15 min, Cell Counting Kit-8 reagent (10 μL) was supplied to the cells followed by incubation of the resultant mixture at 37 °C under 5% CO_2 for 1 h. An analogous cell sample without UV exposure was likewise prepared under conditions otherwise identical to the above procedures. The cell samples thus prepared were subjected to absorption spectroscopy (λ = 450 nm).

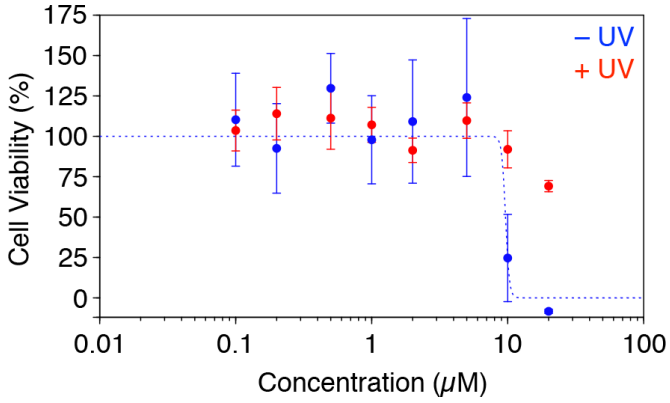

Figure S15. Viabilities of DU145 cells after 15 min incubation in RPMI1640 (0.5% FBS) containing ^{PC}Glue-NBD (0.1–20 μM) before (blue) and after (red) 2 min UV exposure at 365 nm (1.1 mW/mm^2).

11. Surface Charge of Hepatocyte Growth Factor

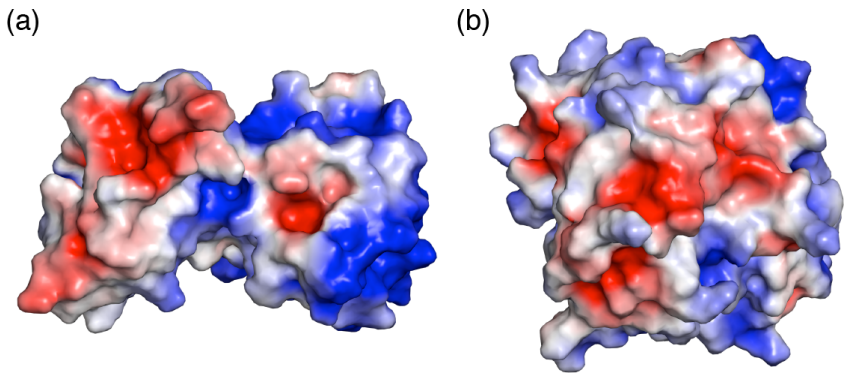

Figure S16. Surface charge distributions of (a) $NK1^{S8}$ and (b) SP^{S9} domains of HGF (red: negative, blue: positive).

12. References

S1. Okuro, K.; Kinbara, K.; Tsumoto, K.; Ishii, N.; Aida, T. Molecular Glues Carrying Multiple Guanidinium Ion Pendants via an Oligoether Spacer: Stabilization of Microtubules against Depolymerization. *J. Am. Chem. Soc.* **2009**, *131*, 1626–1627.

S2. Dcona, M. M.; Mitra, D.; Goehe, R. W.; Gewirtz, D. A.; Lebman, D. A.; Hartman, M. C. T. Photocaged permeability: a new strategy for controlled drug release. *Chem. Commun.* **2012**, *48*, 4755–4757.

S3. Arisaka, A.; Mogaki, R.; Okuro, K.; Aida, T. Caged Molecular Glues as Photoactivatable Tags for Nuclear Translocation of Guests in Living Cells. *J. Am. Chem. Soc.* **2018**, *140*, 2687–2692.

S4. Hill, A. V. A new mathematical treatment of changes of ionic concentration in muscle and nerve under the action of electric currents, with a theory as to their mode of excitation. *J. Physiol.* **1910**, *40*, 190–224.

S5. Goutelle, S.; Maurin, M.; Rougier, F.; Barbaut, X.; Bourguignon, L.; Ducher, M.; Maire, P. The Hill equation: a review of its capabilities in pharmacological modelling. *Fundam. Clin. Pharmacol.* **2008**, *22*, 633–648.

S6. Smith, P. K.; Krohn, R. I.; Hermanson, G. T.; Mallia, A. K.; Gartner, F. H.; Provenzano, M. D.; Fujimoto, E. K.; Goeke, N. M.; Olson, B. J.; Klenk, D. C. Measurement of protein using bicinchoninic acid. *Anal. Biochem.* **1985**, *150*, 76–85.

S7. Ueki, R.; Atsuta, S.; Ueki, A.; Sando, S. Nongenetic Reprogramming of the Ligand Specificity of Growth Factor Receptors by Bispecific DNA Aptamers. *J. Am. Chem. Soc.* **2017**, *139*, 6554–6557.

S8. Modified image of 2QJ2: Tolbert, W. D.; Daugherty, J.; Gao, C.; Xie, Q.; Miranti, C.; Gherardi, E.; Vande Woude, G.; Xu, H. E. A mechanistic basis for converting a receptor tyrosine kinase agonist to an antagonist. *Proc. Natl. Acad. Sci. U. S. A.* **2007**, *104*, 14592–14597. Created with PyMOL 1.8.

S9. Modified image of 4K3J: Merchant, M.; Ma, X.; Maun, H. R.; Zheng, Z.; Peng, J.; Romero, M.; Huang, A.; Yang, N. Y.; Nishimura, M.; Greve, J.; Santell, L.; Zhang, Y. W.; Su, Y.; Kaufman, D. W.; Billeci, K. L.; Mai, E.; Moffat, B.; Lim, A.; Duenas, E. T.; Phillips, H. S.; Xiang, H.; Young, J. C.; Vande Woude, G. F.; Dennis, M. S.; Reilly, D. E.; Schwall, R. H.; Starovasnik, M. A.; Lazarus, R. A.; Yansura, D. G. Monovalent antibody design and

mechanism of action of onartuzumab, a MET antagonist with anti-tumor activity as a therapeutic agent. *Proc. Natl. Acad. Sci. U. S. A.* **2013**, *110*, E2987–E2996. Created with PyMOL 1.8.